Check for updates

Crystallisation in printed droplets: understanding crystallisation of D-mannitol polymorphs†

Asma Buanz, [iD] * Monica Gurung and Simon Gaisford [iD]

Crystallisation of mannitol in the confinement of inkjet printed droplets was studied; the effects of droplet size and the presence of a foreign surface were investigated in comparison to the commonly used manufacturing technique of spray drying. Only the metastable polymorphs (α and δ) were observed in printed droplets with predominance of the α polymorph with increasing the droplet size, except for the smallest droplets generated (~100 pL) where the stable β polymorph was observed. The β polymorph was also predominant in spray-dried samples, with metastable forms appearing upon the addition of a polymer (Eudragit). We propose a dependence of the crystallisation of mannitol polymorphs on either the presence or absence of a surface to favour either the stable or the metastable polymorphs. These findings expand the experimental work that could be conducted to understand the crystallisation behaviour in droplets. By proposing heterogeneous nucleation to favour the formation of the metastable polymorphs while homogeneous nucleation favouring the stable β polymorph, one might understand why the same manufacturing method such as spray drying would produce one polymorph when processed alone but another when present in a formulation. This is of great importance to the pharmaceutical industry to aid in understanding the implications of crystallisation in manufacturing processes such as spray drying.

1. Introduction

Understanding crystallisation behavior of solid materials is key for various industries ranging from food to electronics.[1,2] This is especially evident for the pharmaceutical industry, where the presence of various possible polymorphic and pseudopolymorphic forms that could result from crystallisation can affect not just the performance of the final product but also the intellectual property for that product as well as satisfying regulatory requirements.[3–5]

Crystallisation processes involve two main components: nucleation and crystal growth.[6–8] Depending on the presence or absence of foreign particles or surfaces, nucleation can be either homogeneous or heterogeneous. In the former, the probability of nucleation to be homogeneous across the system is high while in the latter there is a higher chance of the nucleation to occur around foreign bodies. This is due to the reduction of the energy barrier to nucleation when a foreign surface is present, resulting in an enhanced nucleation rate.[7,8] Thus, the presence of a foreign surface can alter the

nucleation mechanism, which generally has a positive effect by increasing the nucleation rate. Foreign particles could also have a negative effect on nucleation if the nucleation on the surface of these particles reduces the effective surface available for the incorporation of growth units, which would result in a net reduction in the nucleation rate.[7]

The effect of foreign particles on nucleation can be increased by either maximising the interaction between the crystallising phase and the surface of the particles, increasing the relative size of the foreign particles or both. This would be highly relevant in the case of crystallisation in confinement where the effect of foreign surfaces is enhanced by the increased area of surface interaction.[9] Understanding such an effect would help explain the behavior of materials in industrial processes that involve both generation of small droplets (confinement) and the presence or lack of solid surfaces (foreign surfaces) such as spray drying (where a solution of an active pharmaceutical ingredient (API) and excipients is dried while being suspended in hot air or gas). This might favour the formation of one polymorphic form over others.[10] Comparing crystallisation behavior of one component (say an API or an excipient) when processed alone and then applying this understanding to that of the material in a formulation can be misleading, as foreign surfaces could also be the API or the excipients used in the formulation.[8] This is in addition to other factors involved such as the mode and rate of supersaturation generation and contact time with foreign surfaces.[7]

UCL School of Pharmacy, University College London, 29-39 Brunswick Square, London, WC1N 1AX, UK. E-mail: asma.buanz.11@ucl.ac.uk

An example is D-mannitol, a common pharmaceutical excipient that has three known polymorphic forms; the stable β form (orthorhombic) and the metastable forms α (orthorhombic) and δ (monoclinic).[11] The thermodynamic relationship between these polymorphs has been reported to be as follows: δ (the lowest melting form) is enantiotropically related to β, α and β forms having similar melting points (166 °C and 166.5 °C, respectively) with the β form having a slightly higher enthalpy of fusion (53.5 ± 0.4 versus 52.1 ± 0.9 kJ mol^{-1}) and the two polymorphs are monotropically related, as the density of the β form is 1.5% higher than that of the α form.[12] It has been reported that both thermodynamic and kinetic properties affect the outcome of crystallisation of D-mannitol from aqueous solutions with high dependency on supersaturation.[13] The resulting polymorphic form varies when crystallised by various well-known industrial drying methods. For instance, in aqueous solution the metastable form δ crystallised (with a small amount of α) by freeze drying,[12] while the stable β form was obtained by spray drying.[10,12,14–16] This might suggest that the drying temperature and/or fast evaporation result in the formation of the β form as the fast evaporation rate achieved by spin coating also resulted in the formation of the β form.[17] However, the β form was also obtained by slow evaporation of mannitol aqueous solution while α by slow cooling of 70% ethanolic solution.[11] A concomitant crystallisation of β and δ forms from slow evaporating micro-litre droplets was reported where the amount of the metastable form increased by lowering the relative humidity.[17] When spray dried with proteins the β form predominantly crystallised with some α form in the presence of lysozyme, with the amount of the α form increased with increasing the lysozyme content.[10,15] Freeze drying mannitol with lysozyme solutions also resulted in the formation of the β form with some δ form (not α).[10] From this it appears that crystallisation of mannitol polymorphs is also affected by the presence of additives. But is the nature of these additives important? Or other factors such as the mode and rate of supersaturation generation might be the key to understanding the crystallisation behaviour of mannitol polymorphs? From the examples mentioned above, there are two main observations: (i) prevalence of concomitant crystallisation of mannitol polymorphs and (ii) with methods involving drying small solution droplets such as spray drying, the δ form is not observed, while it appears with freeze drying.

The first point highlights the similarities between the polymorphic forms of mannitol evidenced by numerous reports of the inter-conversion between them. The transformation is even reported in the absence of a solvent such as during ball milling where β converts to α.[18] The study indicated that the conversion of the stable β form to the metastable α form occurs with minimal microstructural modification. This highlights the similarity between the crystal structure of the two polymorphs: they crystallise in the same orthorhombic space group $P2_12_12_1$ (Table S1†), the conformation of the main backbone is identical but there is a difference in the

OH group conformation with hydrogen bonding schemes, although they have the same number of hydrogen bonds per molecule and thus the conversion can be described as displacive transformation where the crystal lattice is deformed rather than broken.[18] The δ form has similar conformation of the main backbone to the other two polymorphs but deviates from the local C_2 symmetry more than the α and β forms in addition to being the most dense polymorph of the three.[11] Furthermore, solvent-mediated transformation is also reported such as rapid solvent-mediated transformation of δ polymorph to the stable β polymorph.[11]

The difference in the resulting polymorphs of mannitol from two very common drying processes in the pharmaceutical industry that are mentioned in the second point emphasises the need to understand the factors that would affect the crystallisation of a specific polymorph. This would aid in providing better control over the crystallisation of pharmaceuticals. Nucleation, the first step of crystallisation, is governed by the formation of the critical nuclei (crystal nuclei of sufficient size) that is driven by supersaturation. This is then followed by crystal growth until the supersaturation is consumed. The difference between crystallisation in the bulk and confinement is that in the bulk unlimited amount of the material is assumed and thus crystallisation is usually controlled by kinetic factors. This makes Ostwald's rule of stages valid where the least stable form crystallises first and then transforms to the more stable forms. Nonetheless, the rule is empirical and not universally followed; although there are attempts to employ it to explain the dependence of phase stability on the size of crystals.[19,20] In confinement the amount of material is limited and decreases as crystals grow. This suggests that crystallisation in confinement can be either kinetically or thermodynamically controlled.[9,21] This could either result in the formation of the stable form or stabilisation of the metastable forms. Chen et al. reported on controlling the crystallisation of drugs such as glycine and mefenamic acid into their stable forms by confinement in microemulsion.[22] Under such conditions crystallisation starts when stable rather than critical nuclei formed.[9,21,22] Other examples include stabilising metastable anthranilic acid form II in nanoporous glass[23] and the glycine β form by nano spray drying and bi-functional self-assembled monolayers.[24]

A key factor in controlling the outcome of crystallisation in confinement is the size. However, this effect could vary depending on the relative stabilities of the polymorphic forms of any given material, with other factors such as solvent mediated transformations adding to the complexity of this effect. Inkjet printing (IJP) provides a flexible and robust way for studying crystallisation in confinement by generating droplets of varying sizes down to the picoliter range with precise deposition on virtually any surface. The well-developed technique was introduced recently to pharmaceutics,[25] with limited reports on using IJP for investigating the crystallisation behaviour of pharmaceuticals. The focus of printing pharmaceuticals with IJP has been on maintaining drugs in the amorphous state to improve their dissolution.[25,29–39]

We have used the technique successfully for the fast preparation of co-crystals[26] and the unstable β glycine polymorph,[27] demonstrating its applicability to study the factors affecting crystallisation in the confinement of the printed droplets. An early work by Melendez et al.[28] showed two polymorphs of prednisolone crystallised from a solvent mixture solution dispensed from a modified office printer onto poly(tetrafluoroethylene)-coated films. Crystallisation of polymers such as poly(ε-caprolactone)[40] or organic semiconductors[41] by IJP was also reported.

Therefore, the aim of this work was to use inkjet printing with changing the size of the printed droplets and the substrate on which droplets are drying to access ranges of experimental parameters that would be difficult to achieve by other methods. For example, to use nanoporous silica or alumina the material needs to be heated to just above its melting point or annealed at a high temperature, which would not be suitable for heat sensitive compounds.[23,42] D-Mannitol was chosen as a model material because of its importance as an excipient commonly used in the pharmaceutical and food industries thus being heavily studied. This is in addition to the complicated relationships between its polymorphs as discussed earlier. A comparison with spray drying was also conducted.

2. Experimental

2.1 Materials

D-Mannitol (99%) was purchased from Alfa Aesar (UK) and Eudragit RS PO was obtained from Evonik Industries (Evonik Röhm GmbH, Germany) and used as received. Solvents used were distilled water, HPLC grade water (Fisher Scientific), and absolute ethanol (Fisher). Substrates used for printing were glass slides (Thermo scientific, Germany) and aluminium foil (Fisher). Slides were cleaned by sonication in 2% v/v cleaning solution (Micro-90® concentrated cleaning solution, Sigma Aldrich, USA) for 15–30 minutes, rinsed and sonicated with distilled water for 15–30 minutes then dried in a fan oven at 70 °C.

2.2 Inkjet printing

A Jetlab™ 4XL-A research printing platform (MicroFab technologies Ltd, USA) was used to print droplets onto different substrates. The piezoelectric system allows dispensing of individual and multiple droplets. D-Mannitol solution (0.5 M) in HPLC-grade water was filtered through a 0.45 μm Nalgene™ PTFE filter (Thermo Scientific, USA) and dispensed from a 40 μm nozzle (MJ-AT-01) dispensing device at 300 Hz using a driving voltage of 20 V and a pressure of −0.2 psi above the printing solution. Various numbers (1 to 2000) of droplets were dispensed onto glass slides, aluminium foil or Micromesh™ powder X-ray diffraction (PXRD) mounts. A horizontally mounted camera allowed the observation of printed droplets and calculation of their properties with the dedicated droplet analysis software while a downward-looking camera was used to inspect the printed material. Images of drying droplets collected with the downward-looking camera were used to calculate the crystallisation induction time and droplet diameter change using ImageJ software (Fiji project[43]). Microliter droplets of the filtered solution of 0.5 M D-mannitol in water were placed on glass or aluminium foil using a 20 μL Gilson pipette and were allowed to evaporate at room temperature and humidity until complete dryness.

2.3 Spray drying

Spray drying was performed using a Buchi B-290 mini spray dryer (Buchi Labortechnik, CH-Flawil, Switzerland), used with either an open-system for aqueous solutions or closed-system (Inter Loop B-295 operated at −20 °C) for solutions containing ethanol. Drying and atomising gases were compressed air or nitrogen for open and closed-system, respectively. The spray nozzle used has an inner diameter of 0.7 mm and orifice diameter of 1.5 mm. Solutions were either 0.5 M mannitol in water or mannitol : Eudragit RS PO (at 10, 30, 50, 70 and 90% w/w of polymer of the total dry weight) using the ethanol and water solvent mixture (at 10, 30, 50, 70 and 90% ethanol, respectively). Process parameters used were as follows: drying gas inlet temperature = 120 °C, atomising gas flow = 439 L h^{-1} (30 mm), drying gas flow rate = 36 L min^{-1} (aspiration 100%), liquid feed flow rate = 5 mL min^{-1} (15%), drying gas outlet temperature = 60 °C.

2.4 Raman microscopy

Raman spectra were collected using a Labram 200, Horiba Scientific Ltd, equipped with a HeNe laser operated at 632.8 nm and an Olympus optical microscope. Spectra were collected between 100 and up to 3200 cm^{-1} every 10 seconds, with 4 accumulations using a long working distance objective lens (50×). Data capture was performed using LabSpec5 software. Spectra were collected from droplets of varying sizes and presented from the same droplets in each graph.

2.5 Powder X-ray diffraction

Measurements were performed on a Rigaku MiniFlex 600 diffractometer (Rigaku, Tokyo, Japan), which uses Cu Kα radiation (1.5418 Å) at 40 kV and 15 mA. The patterns were collected in the 2θ range from 3 to 35° at a speed of 2° min^{-1} and a step size of 0.01°. An Oxford Diffraction Xcalibur NovaT X-ray diffractometer (Cu Kα radiation, λ = 1.5418 Å) operated at room temperature was used to collect diffraction data from samples crystallized on the PXRD Micromesh. The sample was mounted using transmission geometry, processed, and scaled using CrysAlisPRO software (Rigaku Oxford Diffraction). The sample was mounted perpendicular to the phi axis and rotated over 360° at 0.25° s^{-1}.

3. Results and discussion

Controlled deposition of droplets of D-mannitol aqueous solution was possible with inkjet printing, allowing the deposition of ~100 pL to larger droplets of up to 200 nL on glass

and aluminium surfaces. Mannitol formed spherulites upon drying as shown in Fig. 1. Physical form analysis was performed to identify the resulting polymorphic forms and to investigate the factors affecting their crystallisation.

Due to the small size of the crystals formed and difficulty in performing standard powder X-ray diffraction (PXRD), Raman microscopy was used instead to identify the polymorphic forms produced as the technique is sensitive to the differences in the lattice vibrations of different polymorphic forms.[44] D-Mannitol polymorphs can be distinguished from their Raman spectra; the characteristic bands for D-mannitol polymorphs are single peaks at 876, 1037 and 1136 cm^{-1} for β, a double peak with maxima at 876 and 887 cm^{-1} and single peaks at 1030, 1130, 1355 cm^{-1} for α, and similarly a double peak at 876 and 887 cm^{-1} with a difference in the intensity ratio, and single peaks at 1054 and 1250 cm^{-1} for δ.[17,45]

The Raman spectra collected from crystals formed in a 100 nL drop printed on a glass slide are depicted in Fig. 1b. They indicate crystallisation of the δ form with evidence of the presence of the α form too. The two metastable polymorphs δ and α also crystallised in all droplets of varying sizes up to 200 nL, with the presence of the α form increased as the droplet size increased (Fig. 1c and S1a†). The formation of the metastable forms of mannitol is consistent with our previous observation of the formation of the metastable β form of glycine by the confinement in printed drops.[27]
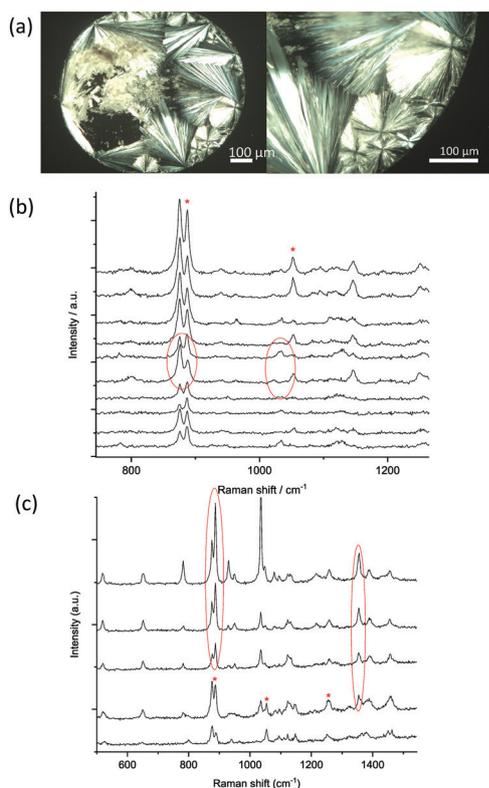
However, in the smallest printed drop of 100 pL, mainly the stable β form of mannitol crystallised as shown from the Raman spectra in Fig. 2.

To collect PXRD data on printed droplets we used an approach we developed before.[27] It involves printing droplets directly onto XRD micromeshes (400 μm in diameter) that are conventionally used to collect small crystal form solutions. The SEM images of mannitol crystals formed in a 10 nL drop printed onto the XRD mesh are shown in Fig. 3a and the PXRD patterns are depicted in Fig. 3b.

A similar behaviour was observed on the aluminium surface, where both α and δ polymorphs crystallised. Nonetheless, the appearance of the α form was observed in larger droplets rather than on glass (Fig. S1b†). The two substrates used, glass and aluminium, have different hydrophilicity resulting in different contact angles as shown in Fig. 4a, with average values of 37.4 ± 1.8° and 79.1 ± 0.7° on glass and aluminium, respectively (measured for water).

The behaviour of the droplet once in contact with the surface is also different which could be measured by the change in droplet diameter with time. This change can reflect on the hysteresis of printed drops on solid substrates.[46] Depicted in Fig. 4b is the change of drop diameter up to the start of crystallisation (i.e. during the crystallisation induction period). The average change was 20.9 ± 9.3% on glass and only 5.2 ± 7.3% on aluminium. There was no clear correlation between the drop size and the degree of this change. This change was not significantly different with the droplet size on aluminium ($p < 0.05$). The value of the contact angle and the level of wetting of that surface reflect the spreading of droplets on substrates. Thus, the lower the value of the contact angle the higher the wetting and the higher the degree of the droplet diameter change during the droplet drying process.

Crystallisation appears to start from the edge of the drops (contact line) as shown in Fig. 5a, with clear formation of the


Fig. 1 (a) PLM images of mannitol crystals in a 100 nL droplet printed on a glass slide, (b) and (c) Raman spectra from crystals formed in 100 and 200 nL droplets (the star indicates the band characteristic of the δ form and the circle indicates the band characteristic of the α form).
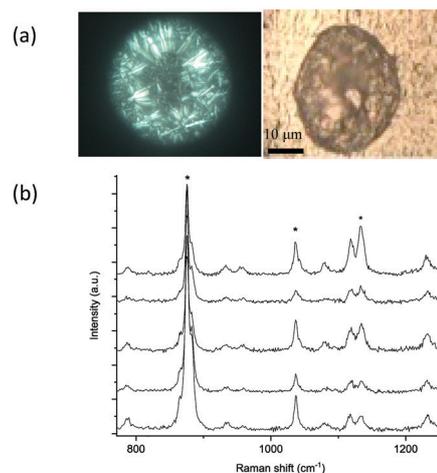
Fig. 2 (a) Images of single droplets on glass (left) and aluminium (right) and (b) Raman mapping results for one single 100 pL droplet on aluminium (stars indicate characteristic bands for the β polymorph).
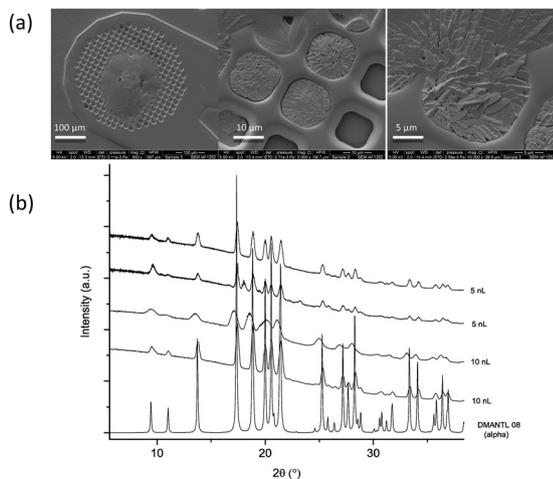
Fig. 3 (a) SEM images of crystals formed in printed droplets on an XRD mesh (10 nL) and (b) XRD patterns for crystals formed in printed 5 and 10 nL droplets showing characteristic peaks for the α polymorph (calculated reference PXRD patterns for mannitol polymorphs are given in Fig. S2†).
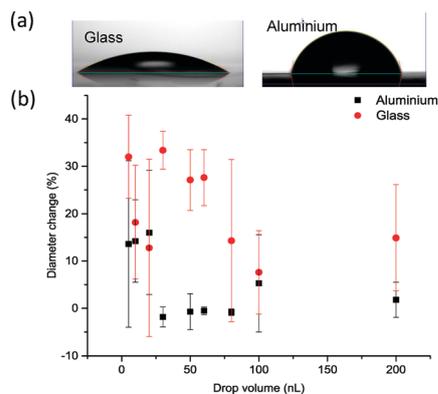
Fig. 4 (a) Lateral images of a drop of water on glass and aluminium substrates and (b) change of the diameter up to the start of crystallisation of printed drops as a function of drop size.

Fig. 5 (a) Images of 100 nL droplets on glass and aluminium foil substrates with the red arrow indicating the point of start of crystallisation and red dotted-line circles indicating coffee-ring formation during droplet drying, and (b) crystallisation induction time as a function of drop volume in droplets printed on both substrates.

coffee-ring effect, where crystals are deposited around the circumference of the dried droplet. As the droplet dries, the rate of evaporation at the edge is fastest and the droplet's contact line is pinned by a capillary flow. This guarantees the replacement of the evaporated liquid from the edges by the liquid from the bulk of the drop. As a result, the dissolved material will be carried by capillary flow to the edge. This means that as the droplet dries the concentration of the solute increases at the edge, generating a region with a higher degree of supersaturation than in the bulk[47] (further images are provided in Fig. S3 and Videos VS1–VS3†). The induction time increased linearly with the increase in the droplet size on both substrates (Fig. 5b), although the evaporation rate increased with increasing droplet size (Fig. S4†). Thus the induction time increased as a result of the increased flow of the solvent to the edge of the droplet. What is more, crystallisation was faster on glass, which correlates well with

the mode of droplet spreading on the two substrates as more spreading (higher % of droplet diameter change) results in faster evaporation and thus faster crystallisation (*i.e.* shorter crystallisation induction time).

The largest droplet size studied by printing was 200 nL (made out of 2000 droplets printed in microseconds on one spot). To study crystallisation in droplets in the microliter range, they were micro-pipetted onto the substrates. Characteristic peaks for α and δ polymorphs are observed in crystals formed in droplets up to 10 μL on glass slides, which is similar to printed droplets. Raman spectra were also collected during the drying of a 0.2 μL droplet showing only the progression of the appearance of the α polymorph (Fig. S5 and S6†).

To collect PXRD data, microliter drops were also pipetted onto a different type of a PXRD holder (glass holder), which allowed the collection of PXRD data on crystals from microliter droplets. The peaks for α as well as δ polymorphs are observed in all droplets, with peaks for the β form appearing in larger droplets (60 μL) (Fig. S7a and b†).

Concomitant crystallisation of mannitol is a common phenomenon,[48,49] with reports of cross-nucleation especially of the α form.[8] Therefore, competing thermodynamic and kinetic factors results in the concomitant crystallisation of D-mannitol polymorphs. This would favour the nucleation, growth or conversion of one polymorph over the other. The observation of domination of the α form as the drop size

increases could indicate that as the evaporation slowed down a possible conversion of the δ form to the α form occurs. Observing a 10 μL droplet on glass shows clear conversion in crystals following crystallisation while they were still in contact with the remaining solvent (Fig. S8 and Video VS4†). Another explanation would be that the α form favours nucleation on solid surfaces (the surface induced polymorph). This means that the larger the surface the solution is in contact with, the bigger the chance of nucleating the α form. This would explain the formation of this form on both substrate materials used here and why it forms in smaller droplets on glass (more solution spreading) rather than aluminium (less spreading).

It was interesting to notice the β form in both large μL drops and very small (~100 pL) printed drops. This could be explained by two different factors at these droplet sizes extremes; observations of the β form crystallising in bulk solution have been reported, which is consistent with it being the most stable form to which the other polymorphs convert to eventually in the presence of excess solvent (water).[50] On the other hand, the confinement in the very small drop of 100 pL might have caused the relative stability of mannitol polymorphs to change and thus the β form has become metastable and nucleated first, and due to the fast evaporation it did not convert to the now stable forms (α and δ). This could be possible as crystallisation in the confinement of nanopores can result in a change in the stability ranking of polymorphs.[9,51,52] Nonetheless, we do not believe that this is the case here. Another explanation would be that the β form requires homogeneous nucleation, which would be in the absence of surface or foreign particles. In such small droplets the evaporation is very rapid such that the droplet behaves as if there is no surface and thus results in the formation of the β form. From the light microscopy images of single droplets the absence of coffee-ring formation is clear (Fig. 2a), as the convection flow that supplies the edge of the droplet with solute molecules is inhibited at such a small scale,[53] which prevents the formation of the coffee-ring. Convection promotes heterogeneous nucleation and thus factors suppressing convection appear to promote homogeneous nucleation[7] and the absence of this effect possibly encourages homogeneous nucleation, which supports the formation of the β polymorph. We have not been able to measure the supersaturation at the point of nucleation but envisage that this would enhance the understanding of the nature of nucleation of different polymorphs.

Comparison with spray drying

An appropriate comparison would be with a drying method that involves fast evaporation of droplets without the presence of a solid surface. Spray drying was chosen as in this technique the solution is atomised into small droplets directly into a stream of hot air or gas.[54] This provides a fast evaporation of the solvent and thus could be comparable to the evaporation rate in small printed droplets. As the drop-

lets are suspended in hot air or gas, they do not come in contact with any solid surface.

Mannitol was spray dried with and without the presence of a polymer (Eudragit®). Eudragit RS PO is a polymethacrylate-based copolymer that is insoluble in water but soluble in organic solvents,[55] therefore, solutions for spray drying that contained this polymer were prepared with a mixture of water and ethanol. Powder samples were collected and characterised with PXRD and Raman spectroscopy. PXRD results show that only the β form is observed when mannitol was spray dried alone both from water and water and ethanol mixtures (Fig. S9†) and with 10% w/w polymer (Fig. 6). On the other hand, the α form was observed in the sample containing 30% w/w polymer while the δ form appeared in the samples containing 50 and 70% w/w polymer. At 90% w/w polymer content the sample was predominantly amorphous (Fig. 6). The DSC results are consistent with the PXRD results showing a shift of the endothermic transition in the samples with the higher concentration of the polymer to a lower temperature indicating the melting of the δ polymorph (155 °C)[12] (Fig. S10†).

This is consistent with the reports in the literature mentioned earlier of the β form being observed by spray drying of aqueous solutions while adding enzymes to the solution increased the formation of the α form.[15] The enzyme was observed to accumulate on the surface of the particles and thus
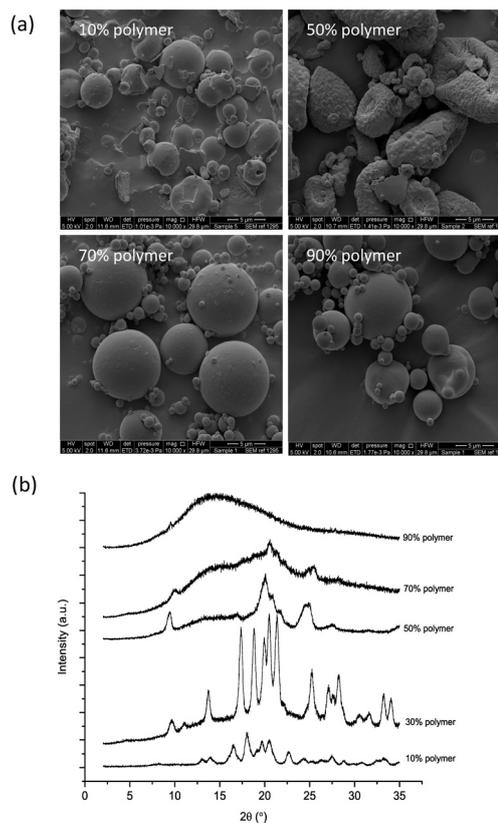

Fig. 6 a) SEM images and b) PXRD patterns of spray dried mannitol with Eudragit polymer (10 to 90% w/w).

the authors suggest that this slowed down drying by reducing water transportation to the surface. It is not clear though how that would favour the formation of the metastable α form.[15] Another explanation based on our findings from this current study would be that the enzyme acted as a heterogeneous surface for nucleation and thus the α form was preferred, as in the case with printed droplets in our study, while in the absence of the enzyme the β form was favoured.

The size of spray-dried particles was between 2.5 and 15 μm as shown in the SEM images presented in Fig. 6a and S9.† This is smaller than that of the printed droplets in which the β form was observed (60 μm) and could mean that spray drying even larger droplets should still result in the formation of the β form. This has been reported where larger droplets (up to 1.5 mm) were subjected to a similar condition as in spray drying using the solvent levitation method. In this method a single droplet is suspended in an ultrasonic field and in the presence of a drying gas.[15] The β form was observed in these experiments with the presence of the α form. When lysozyme was introduced the amount of the α form increased until the higher concentration of the enzyme β form was not observed. This is consistent with our hypothesis that the presence of a foreign particle or surface favours the nucleation of the α form, as well as it is being the fast growing polymorph among mannitol polymorphs, while the β form is preferred in the absence of a heterogeneous surface. The latter is consistent with the observation of either the α or δ form from the melt but never β.[56,57]

This does not rule out the possibility of the crystallisation of the β form and then converting to α or δ forms in such large (microliter) droplets, as real time identification of the polymorphic forms as the printed droplet where drying was not possible, especially with Raman microscopy as the signal was too weak in the presence of the solvent. This could be ruled out in smaller droplets where evaporation is very fast that chances of solvent-mediated transformation are very low. The air–water interface appears to play an important role in crystallisation from both printed and spray dried droplets. The role of this interface in the crystallisation and denaturation of proteins in spray-dried droplets has been investigated[58] but further work is required to improve understanding of its role in the crystallisation of small molecules.

4. Conclusions

Inkjet printing allows very fine control over droplet size, which enabled the study of the crystallisation behaviour of D-mannitol's closely related polymorphs. In summary (i) the confinement in the smallest printed droplets of *ca.* 100 pL favoured the formation of the stable β form, (ii) larger droplets in nL size range promoted the crystallisation of the metastable forms with fast evaporation possibly prevented solvent-mediated transformation to the stable form and (iii) slow evaporation in microliter droplets resulted in the crystallisation of β and the least stable δ form. Evidence sug-

gests that the α polymorphs favour nucleation on the solid surface.

The findings from spray drying indicate that confinement within sprayed droplets and the very fast evaporation rate favoured the formation of the β form despite the droplet size being larger than that of the printed ones where the β form was obtained (μL *versus* pL). Spray drying with a polymer appears to favour the formation of the metastable form α, which supports the hypothesis of it being a surface-induced polymorph. Further work is required to provide clearer evidence on the nature of the nucleation being either homogeneous or heterogeneous. This also highlights the applicability of inkjet printing in investigating crystallisation in confinement which can help understand the crystallisation behaviour in commonly used manufacturing techniques such as spray drying. It also aids in studying general crystallisation in thin films to much smaller droplets as usually larger droplets are studied. In addition, studying crystallisation in confinement with printing is different from other approaches where heating is required, such as with confinement in nanoporous materials, which is not suitable for heat-sensitive materials.

Conflicts of interest

There are no conflicts to declare.

Acknowledgements

Notes and references

1 A. J. Florence, A. Johnston, S. L. Price, H. Nowell, A. R. Kennedy and N. Shankland, *J. Pharm. Sci.*, 2006, **95**, 1918–1930.
2 A. O. F. Jones, B. Chattopadhyay, Y. H. Geerts and R. Resel, *Adv. Funct. Mater.*, 2016, **26**, 2233–2255.
3 S. Byrn, R. Pfeiffer, M. Ganey, C. Hoiberg and G. Poochikian, *Pharm. Res.*, 1995, **12**, 945–954.
4 A. J. Alvarez, A. Singh and A. S. Myerson, *Cryst. Growth Des.*, 2009, **9**, 4181–4188.
5 J. Haleblian and W. McCrone, *J. Pharm. Sci.*, 1969, **58**, 911–929.
6 J. Bernstein, R. J. Davey and J.-O. Henck, *Angew. Chem., Int. Ed.*, 1999, **38**, 3440–3461.
7 X. Y. Liu, *J. Chem. Phys.*, 2000, **112**, 9949–9955.
8 J. Tao, K. J. Jones and L. Yu, *Cryst. Growth Des.*, 2007, 7, 2410–2414.
9 Q. Jiang and M. D. Ward, *Chem. Soc. Rev.*, 2014, **43**, 2066–2079.
10 H. Grohganz, Y.-Y. Lee, J. Rantanen and M. Yang, *Int. J. Pharm.*, 2013, **447**, 224–230.
11 H. N. Kamel, F. R. Fronczek and M. Slattery, *Acta Crystallogr., Sect. C: Cryst. Struct. Commun.*, 2003, **59**, o567–o570.

12 A. Burger, J.-O. Henck, S. Hetz, J. M. Rollinger, A. A. Weissnicht and H. Stöttner, *J. Pharm. Sci.*, 2000, **89**, 457–468.

13 W. Su, H. Hao, B. Glennon and M. Barrett, *Cryst. Growth Des.*, 2013, **13**, 5179–5187.

14 Y.-Y. Lee, J. X. Wu, M. Yang, P. M. Young, F. van den Berg and J. Rantanen, *Eur. J. Pharm. Sci.*, 2011, **44**, 41–48.

15 J. P. Pajander, S. Matero, J. Sloth, F. Wan, J. Rantanen and M. Yang, *Pharm. Res.*, 2015, **32**, 1993–2002.

16 S. G. Maas, G. Schaldach, E. M. Littringer, A. Mescher, U. J. Griesser, D. E. Braun, P. E. Walzel and N. A. Urbanetz, *Powder Technol.*, 2011, **213**, 27–35.

17 S. K. Poornachary, J. V. Parambil, P. S. Chow, R. B. H. Tan and J. Y. Y. Heng, *Cryst. Growth Des.*, 2013, **13**, 1180–1186.

18 P. Martinetto, P. Bordet, M. Descamps, E. Dudognon, W. Pagnoux and J.-F. Willart, *Cryst. Growth Des.*, 2017, **17**, 6111–6122.

19 D. Zahn and J. Anwar, *Chem. – Eur. J.*, 2011, **17**, 11186–11192.

20 G. T. Rengarajan, D. Enke, M. Steinhart and M. Beiner, *Phys. Chem. Chem. Phys.*, 2011, **13**, 21367–21374.

21 C. E. Nicholson, C. Chen, B. Mendis and S. J. Cooper, *Cryst. Growth Des.*, 2011, **11**, 363–366.

22 C. Chen, O. Cook, C. E. Nicholson and S. J. Cooper, *Cryst. Growth Des.*, 2011, **11**, 2228–2237.

23 J.-M. Ha, J. H. Wolf, M. A. Hillmyer and M. D. Ward, *J. Am. Chem. Soc.*, 2004, **126**, 3382–3383.

24 X. Yang and A. S. Myerson, *CrystEngComm*, 2015, **17**, 723–728.

25 R. Daly, T. S. Harrington, G. D. Martin and I. M. Hutchings, *Int. J. Pharm.*, 2015, **494**, 554–567.

26 A. B. M. Buanz, R. Telford, I. J. Scowen and S. Gaisford, *CrystEngComm*, 2013, **15**, 1031–1035.

27 A. B. M. Buanz and S. Gaisford, *Cryst. Growth Des.*, 2017, **17**, 1245–1250.

28 P. A. Melendez, K. M. Kane, C. S. Ashvar, M. Albrecht and P. A. Smith, *J. Pharm. Sci.*, 2008, **97**, 2619–2636.

29 N. Scoutaris, *PhD thesis*, University of Nottingham, 2010.

30 N. Sandler, A. Maattanen, P. Ihalainen, L. Kronberg, A. Meierjohann, T. Viitala and J. Peltonen, *J. Pharm. Sci.*, 2011, **100**, 3386–3395.

31 N. Scoutaris, M. R. Alexander, P. R. Gellert and C. J. Roberts, *J. Controlled Release*, 2011, **156**, 179–185.

32 N. Genina, D. Fors, H. Vakili, P. Ihalainen, L. Pohjala, H. Ehlers, I. Kassamakov, E. Haeggström, P. Vuorela, J. Peltonen and N. Sandler, *Eur. J. Pharm. Sci.*, 2012, **47**, 615–623.

33 A. Kamyshny and S. Magdassi, in *Inkjet-Based Micromanufacturing*, Wiley-VCH Verlag GmbH & Co. KGaA, 2012, pp. 173–189, DOI: 10.1002/9783527647101.ch12.

34 N. Genina, D. Fors, M. Palo, J. Peltonen and N. Sandler, *Int. J. Pharm.*, 2013, **453**, 488–497.

35 N. Genina, E. M. Janßen, A. Breitenbach, J. Breitkreutz and N. Sandler, *Eur. J. Pharm. Biopharm.*, 2013, **85**, 1075–1083.

36 R. Kolakovic, T. Viitala, P. Ihalainen, N. Genina, J. Peltonen and N. Sandler, *Expert Opin. Drug Delivery*, 2013, **10**, 1711–1723.

37 R. D. Boehm, P. R. Miller, J. Daniels, S. Stafslien and R. J. Narayan, *Mater. Today*, 2014, **17**, 247–252.

38 M. Robin, W. Kuai, M. Amela-Cortes, S. Cordier, Y. Molard, T. Mohammed-Brahim, E. Jacques and M. Harnois, *ACS Appl. Mater. Interfaces*, 2015, **7**, 21975–21984.

39 M. Scarpa, S. Stegemann, W.-K. Hsiao, H. Pichler, S. Gaisford, M. Bresciani, A. Paudel and M. Orlu, *Int. J. Pharm.*, 2017, **523**, 327–335.

40 N. Sanandaji, A. Oko, D. B. Haviland, E. A. Tholén, M. S. Hedenqvist and U. W. Gedde, *Eur. Polym. J.*, 2013, **49**, 203–208.

41 H. Minemawari, T. Yamada, H. Matsui, J. y. Tsutsumi, S. Haas, R. Chiba, R. Kumai and T. Hasegawa, *Nature*, 2011, **475**, 364–367.

42 E. Woo, J. Huh, Y. G. Jeong and K. Shin, *Phys. Rev. Lett.*, 2007, **98**, 136103.

43 J. Schindelin, I. Arganda-Carreras, E. Frise, V. Kaynig, M. Longair, T. Pietzsch, S. Preibisch, C. Rueden, S. Saalfeld, B. Schmid, J.-Y. Tinevez, D. J. White, V. Hartenstein, K. Eliceiri, P. Tomancak and A. Cardona, *Nat. Methods*, 2012, **9**, 676–682.

44 A. Paudel, D. Raijada and J. Rantanen, *Adv. Drug Delivery Rev.*, 2015, **89**, 3–20.

45 W. Su, H. Hao, M. Barrett and B. Glennon, *Org. Process Res. Dev.*, 2010, **14**, 1432–1437.

46 M. Rein, *Fluid Dyn. Res.*, 1993, **12**, 61–93.

47 R. D. Deegan, O. Bakajin, T. F. Dupont, G. Huber, S. R. Nagel and T. A. Witten, *Nature*, 1997, **389**, 827–829.

48 D. E. Braun, S. G. Maas, N. Zencirci, C. Langes, N. A. Urbanetz and U. J. Griesser, *Int. J. Pharm.*, 2010, **385**, 29–36.

49 J. Cornel, P. Kidambi and M. Mazzotti, *Ind. Eng. Chem. Res.*, 2010, **49**, 5854–5862.

50 B. O'Sullivan and B. Glennon, *Org. Process Res. Dev.*, 2005, **9**, 884–889.

51 B. D. Hamilton, J.-M. Ha, M. A. Hillmyer and M. D. Ward, *Acc. Chem. Res.*, 2012, **45**, 414–423.

52 M. D. Ward, *Isr. J. Chem.*, 2017, **57**, 82–91.

53 M. R. Barmi and C. D. Meinhart, *J. Phys. Chem. B*, 2014, **118**, 2414–2421.

54 R. Vehring, *Pharm. Res.*, 2008, **25**, 999–1022.

55 S. Thakral, N. K. Thakral and D. K. Majumdar, *Expert Opin. Drug Delivery*, 2013, **10**, 131–149.

56 J. Tao and L. Yu, *J. Phys. Chem. B*, 2006, **110**, 7098–7101.

57 L. Yu, *J. Am. Chem. Soc.*, 2003, **125**, 6380–6381.

58 Y.-F. Maa, P.-A. T. Nguyen and S. W. Hsu, *J. Pharm. Sci.*, 1998, **87**, 152–159.